NRO APPROVED FOR RELEASE
DECLASSIFIED BY: C/IART
DECLASSIFIED ON: 9 JULY 2012

Logged

~~SECRET~~ SPECIAL HANDLING

AC-04306
VOLUME III
31 March 1965
Copy No. 3

[redacted]

Quill

RADAR

HANDLE VIA [illegible]
CONTROL SYSTEM ONLY

PROGRAM [redacted]

VEHICLE 2355 SYSTEM REPORT (U)

VOLUME III – FLIGHT PERFORMANCE

☐ RT DATA ENTERED
DATE ____________
☐ MICROFICHED
DATE ____________

Quill

BYE 36454/65

SAFSS ~~5H0417-65~~

Vol III
P-12 498
cy 3

HANDLE VIA [illegible]
CONTROL [illegible] ONLY

~~SECRET~~ SPECIAL HANDLING

LOCKHEED MISSILES & SPACE COMPANY

AC-04306
Volume III
31 March 1965

Copy No. 3
120 Sheets

S

BYE-36454/65 3VOL3N

PROGRAM [redacted]

VEHICLE 2355 SYSTEM REPORT (U)

Volume III - Flight Performance

Contract [redacted]
Supplemental Agreement Number 13

Quill

Prepared:

[redacted]

[redacted]
Chief Operations
Program [redacted]

Approved:

[redacted]

[redacted]
Manager
Program [redacted]

Approved:

~~David D. Bradburn~~

David D. Bradburn
Lt. Colonel, USAF
SAFSP

BYE 36454/65

HANDLE VIA [illegible] CONTROL SYSTEM ONLY.

FOREWORD

This report covers the span of time from the inception of the first satellite borne radar system through the final evaluation of the on orbit performance of the first flight. An objective review is attempted, of the complete scope of activities associated with bringing a new system into being and of the system performance during an essentially nominal and troublefree mission.

From this review, it is hoped that the systems management and program control parameters which were found to be effective may be properly recognized and thereby enhance the organization and conduct of similar future activities.

The system definition and resulting configuration is reviewed in retrospect, together with the problems associated with this Program development and testing.

The engineering management concept and the test philosophy which were applied are outlined and restated, with the objectives of first recording these, and then attempting to objectively analyze them for areas susceptible to improvement. The Air Force - LMSC - Associate Contractor team is defined, as it existed during the development, testing and operation of Vehicle 2355.

The system performance from launch through recovery and thence to battery depletion is evaluated from the primary aspect of payload operation.

System performance is compared against predictions, and the performance accomplishments and achievements are enumerated.

The report is therefore, in addition to a flight report, a total summary of the composite effort associated with the preparation and operation of this system. From the system evaluation certain conclusions and recommendations are formulated which are intended to be useful for later work on similar systems.

Through the medium of the detailed information contained in this report, it is intended to properly acknowledge the efforts of all those who were instrumental in managing and conducting a program which produced a completely successful mission with the first flight of a new payload vehicle system.

PART III

Table of Contents

PART III (Cont.)

Table of Contents

AC04306

Report Numbering and Organization

The complete 2355 System Report is contained in three volumes.

Volume I - (PART I) - Summary
Volume II - (PART II) - Engineering
Volume III - (PART III) - Flight Performance

The report paragraph numbering is in accordance with the following convention:

First number indicates volume number
Second number indicates main paragraph number
Third number indicates a subparagraph
Fourth number indicates a further subdivision of a subparagraph

Figures are numbered consecutively within main paragraphs.

Reports By Participating Contractors

The complete system description and performance evaluation is contained in reports issued by the three contractors. These are listed here for reference by the reader:

Lockheed Missiles and Space Company:

Title: 2355 System Report, dated 31 March 1965.

Volume I - Summary
Volume II - Engineering
Volume III - Flight Performance

Goodyear Aerospace Corporation:

Title: Program Report, KP-II Orbital Doppler Radar, Thor/Agena Satellite Program, dated 1 March 1965.

[redacted]

Title: [redacted]

PART III

System Performance During Orbital Operations

Introduction

This section of the report - Part III - is designed to contain a maximum of orbital performance data. The subsystems, the thermodynamic conditions which prevailed, the vacuum gage responses and the performance of the Satellite Control Facility are each discussed.

The payload subsystem operation, as recorded in Para. 3.4, was evaluated by Engineering personnel relatively inexperienced in evaluation of photographs or of radar imagery. The basis of the evaluation was:

- All telemetry data considered pertinent.
- The recorded video data transparency.
- The correlated radar imagery for the full length of all operating passes. (An unrefined copy)

The resulting observations and comments provide a total evaluation of the payload data and radar imagery accumulated in 32.91 minutes of operation throughout the 14 orbits of payload operation - with the qualifications indicated above.

The entries made for each pass may form a basis for further evaluation - if required - without recourse to extensive research through retired data records.

3.1 Electrical Power Subsystem

3.1.1 Summary

The 2355 Electrical Power System performed flawlessly throughout the entire mission. Ascent, orbit, recovery, and post-recovery orbital performance of all components was normal until the rated capacity of the three Type 1-D batteries had been exhausted, at Orbit 73. Abnormal loads on the output of the High Voltage Power Supply occurred during payload operation on Orbits 8 and 9; however, no interruptions or excessive degradation in output from the power supply was present. The abnormal high voltage loads at Orbits 8 and 9 were of two types, each identical in all respects to similar disturbances experienced during payload testing in the TASC Chamber, 30 November 1964.

3.1.2 Battery Performance

Battery performance was exceptional for the duration of the mission. Average current division throughout the life of the vehicle was 2:1 as anticipated, within the tolerance of the Ampere Hour Meters (+0, -10 ampere-hours). Projected versus actual AHM readings are shown in Fig. 3.1.1. Actual values are slightly lower than predicted because of: a) the AHM tolerance, b) relatively early recovery, and c) the fact that actual average payload operation was conducted at PRF Step 8 or 9, rather than at PRF Step zero (worst case) for which the projections were made.

Battery temperatures increased slowly throughout the mission. All three Type 1-D batteries were between 65° and 75° from launch to recovery, and from 73° to 85°F from recovery to Orbit 73.

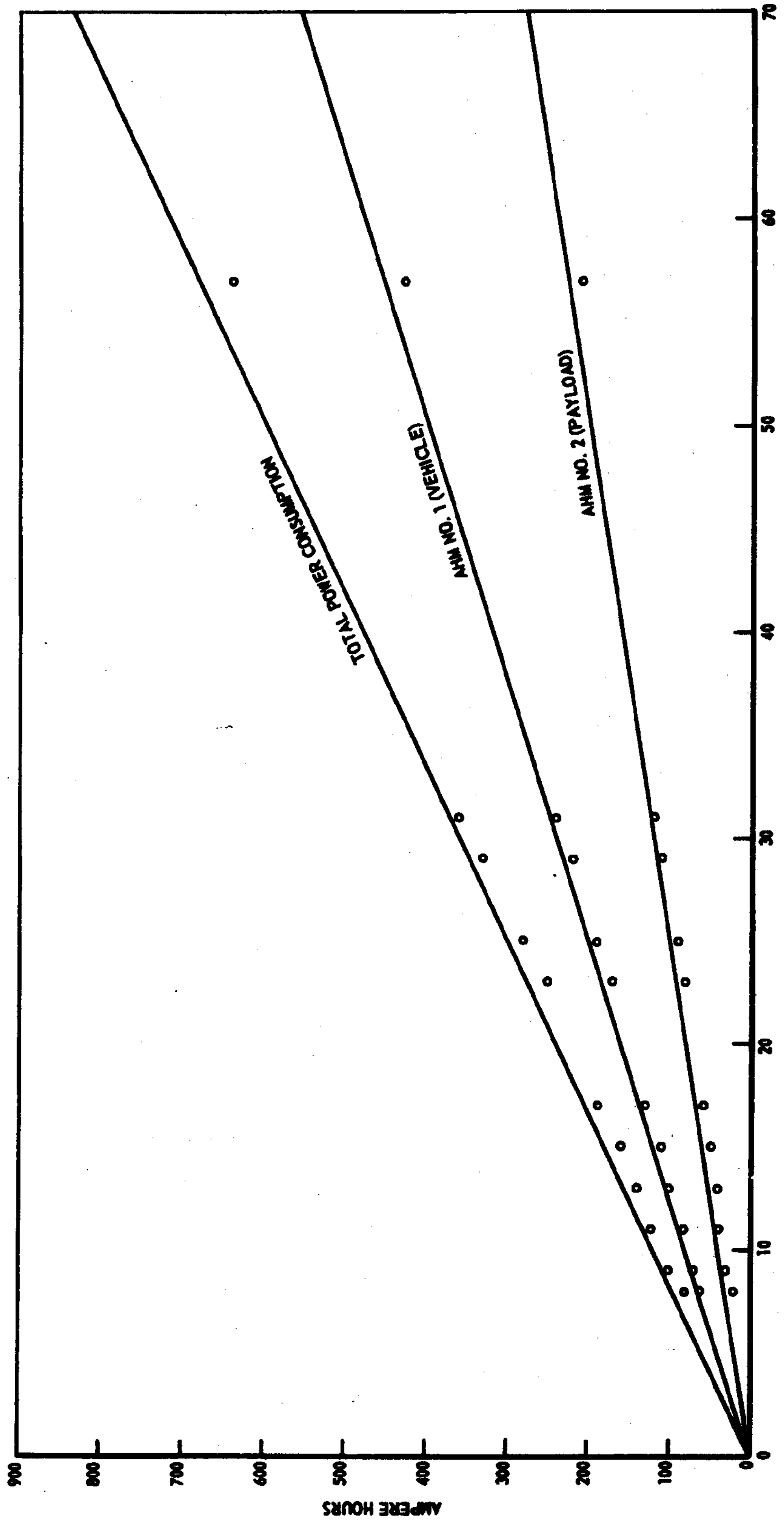

Figure 3.1.1 Predicted Ampere Hour Meter Readings - Vehicle 2355 Actual Values are Shown (o)

3.1.3 Power Conversion Equipment Performance

Vehicle and Payload Power Conversion Equipment performance was normal throughout the flight. The switching of the payload conversion equipment was executed as programmed. All output voltages were within specification except during payload operation on the last payload operating pass, Orbit 72. During this pass, the batteries were nearly expended and the internal resistance was relatively high. For this reason, the battery voltage dropped below 22 volts during the high-current payload operating period causing the Power Conversion Equipment to fail to regulate properly. The low buss voltage effect upon the 2 KC inverter was most severe as shown in Table 3.1.1. Payload read-in data was satisfactory during the pass, however, until 22653 seconds System Time when an Attenuator 7 command was sent. As a result of this command, it is impossible to evaluate payload data subsequent to this time. The buss voltage at 22653 seconds when data was lost was 18.6 volts.

3.1.4 Discussion of Abnormal High Voltage Loads at Orbits 8 and 9

Analysis of 2355 flight data indicates a series of high voltage disturbances during the first two payload operating orbits, NHS Pass 8 and VTS Pass 9. The disturbances are of two types: Type I is a brief pulse of excessive high voltage supply output current coincident with a slight decrease in high voltage; Type II is a sustained disturbance, lasting 12 seconds at Orbit 8 (refer to Figures 3.1.2 - 3.1.5). These indications are noticeable by virtue of the amplification and delayed decay characteristics of the peak reading monitors, C-283, and C-284.

TABLE 3.1.1

System Time	22609	22610	22653	22686	22687	22696
Payload Mode	Pre-operate	Operate	Operate	Operate	Warmup	Warmup
Battery Voltage	23.0	20.5	18.6	18.3	20.9	23.0
+28 Reg. (VDC)	28.0	28.0	25.7	25.3	28.3	28.3
2 KC (VAC)	110	100	90	88	105	111
ØAB (VAC)	115	114	105	103	115	115
ØCB (VAC)	115	109	100	98	115	115
ØAC (VAC)	115	115	109	107	115	115

Power Conversion Equipment temperatures were between 61° and 90°F from launch to Orbit 73.

The Type I disturbance occurred 7 times during Orbit 8 and 4 times during Orbit 9. The Type II disturbance occurred only once, at Orbit 8.

The Type II disturbance started at 24268 seconds and stopped at 24280 seconds System Time. The Type II disturbance is characterized by: a) a slight decrease in high voltage; b) a slight decrease in high voltage supply input current; c) essentially constant high voltage supply output current until the end of the disturbance when the current momentarily increases; d) an oscillatory noise burst causing the high voltage peak-reading monitors to repsond. The slight decrease in high voltage is considered to be caused by the effect of the abnormal oscillatory nature of the load at the time of the disturbance on the regulator circuit of the Lear-Siegler unit.

Both types of disturbance discussed here were also encountered during payload altitude testing in the TASC Chamber 30 November 1964, and were present only during the first four simulated orbits.

The source of the disturbances is the transmitter or the power supply. A conclusive finding as to cause cannot be established.

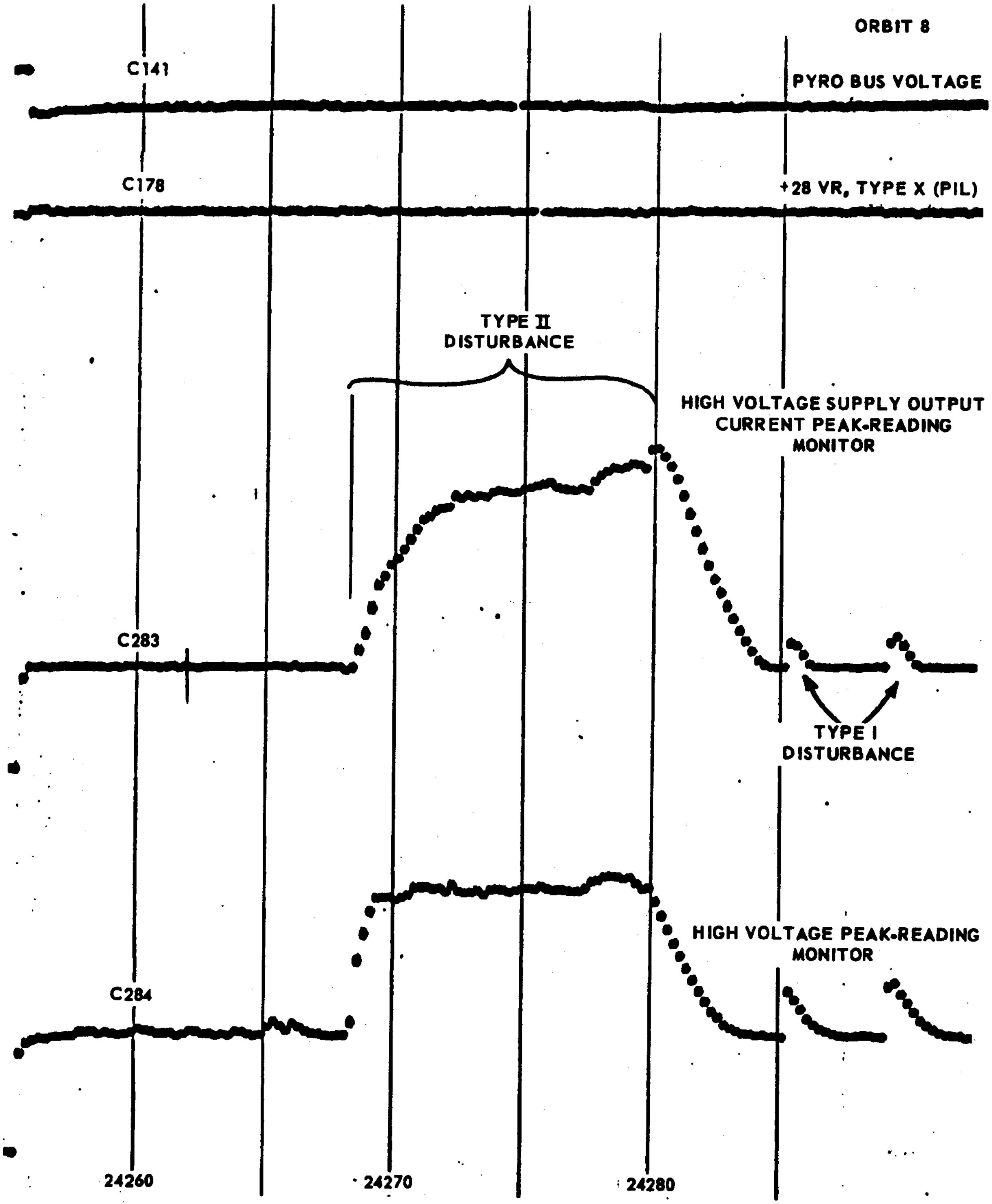
ORBIT 8
C141
PYRO BUS VOLTAGE
C178
+28 VR, TYPE X (PIL)
TYPE II
DISTURBANCE
HIGH VOLTAGE SUPPLY OUTPUT
CURRENT PEAK-READING
MONITOR
C283
TYPE I
DISTURBANCE
HIGH VOLTAGE PEAK-READING
MONITOR
C284
24260
24270
24280

Figure 3.1.2

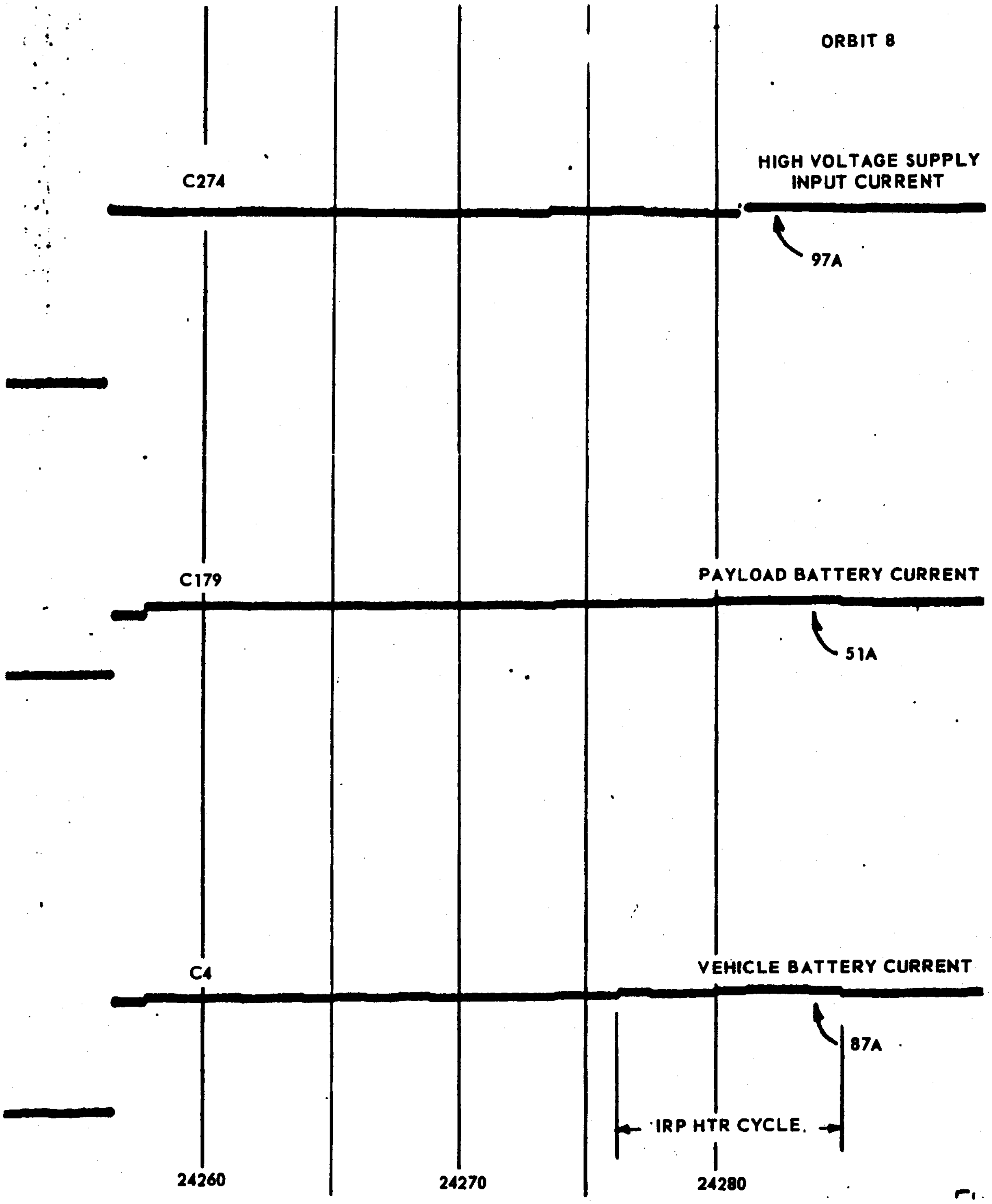
ORBIT 8
C274
HIGH VOLTAGE SUPPLY INPUT CURRENT
97A
C179
PAYLOAD BATTERY CURRENT
51A
C4
VEHICLE BATTERY CURRENT
87A
IRP HTR CYCLE
24260
24270
24280

Figure 3.1.3

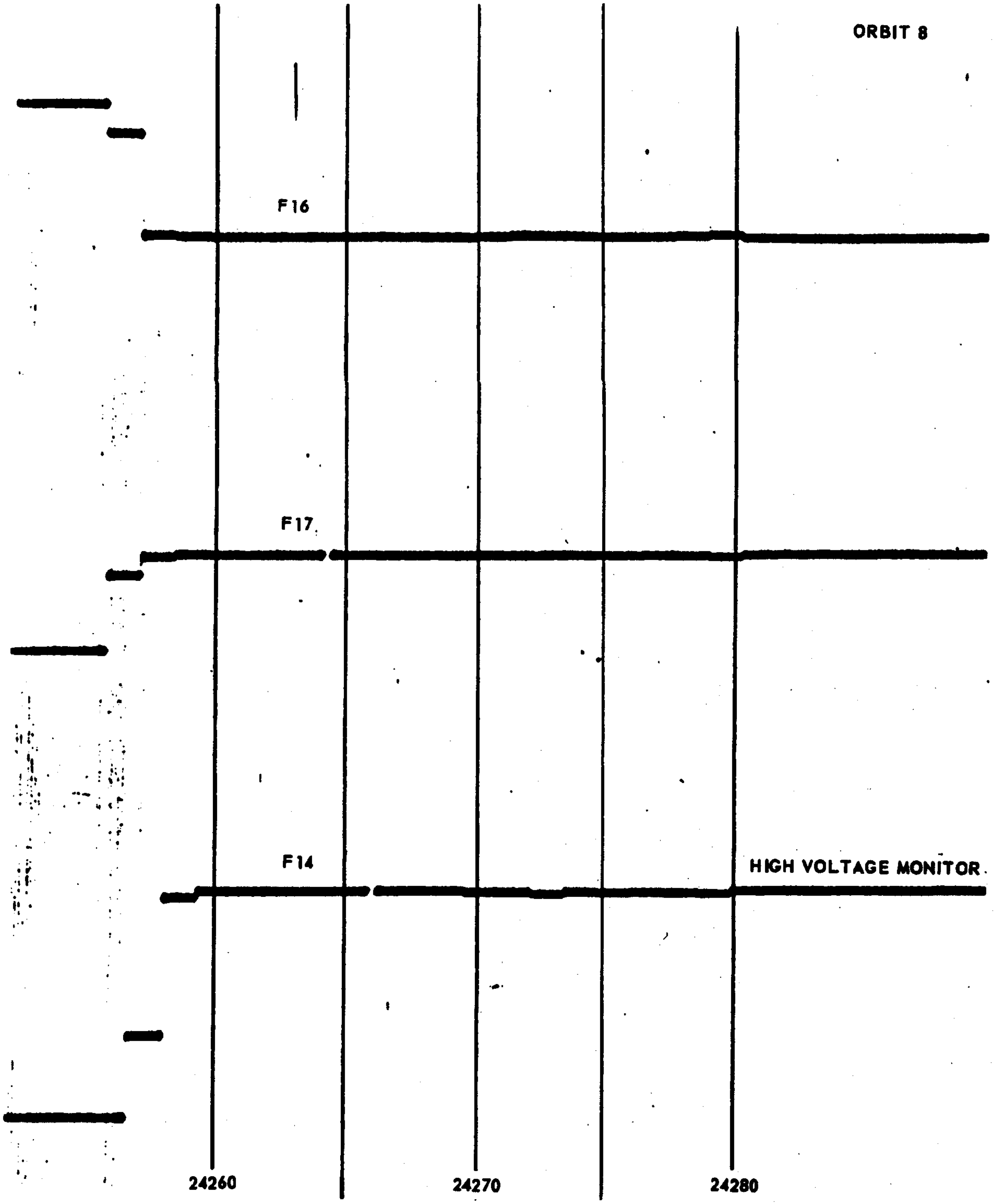

Figure 3.1.4

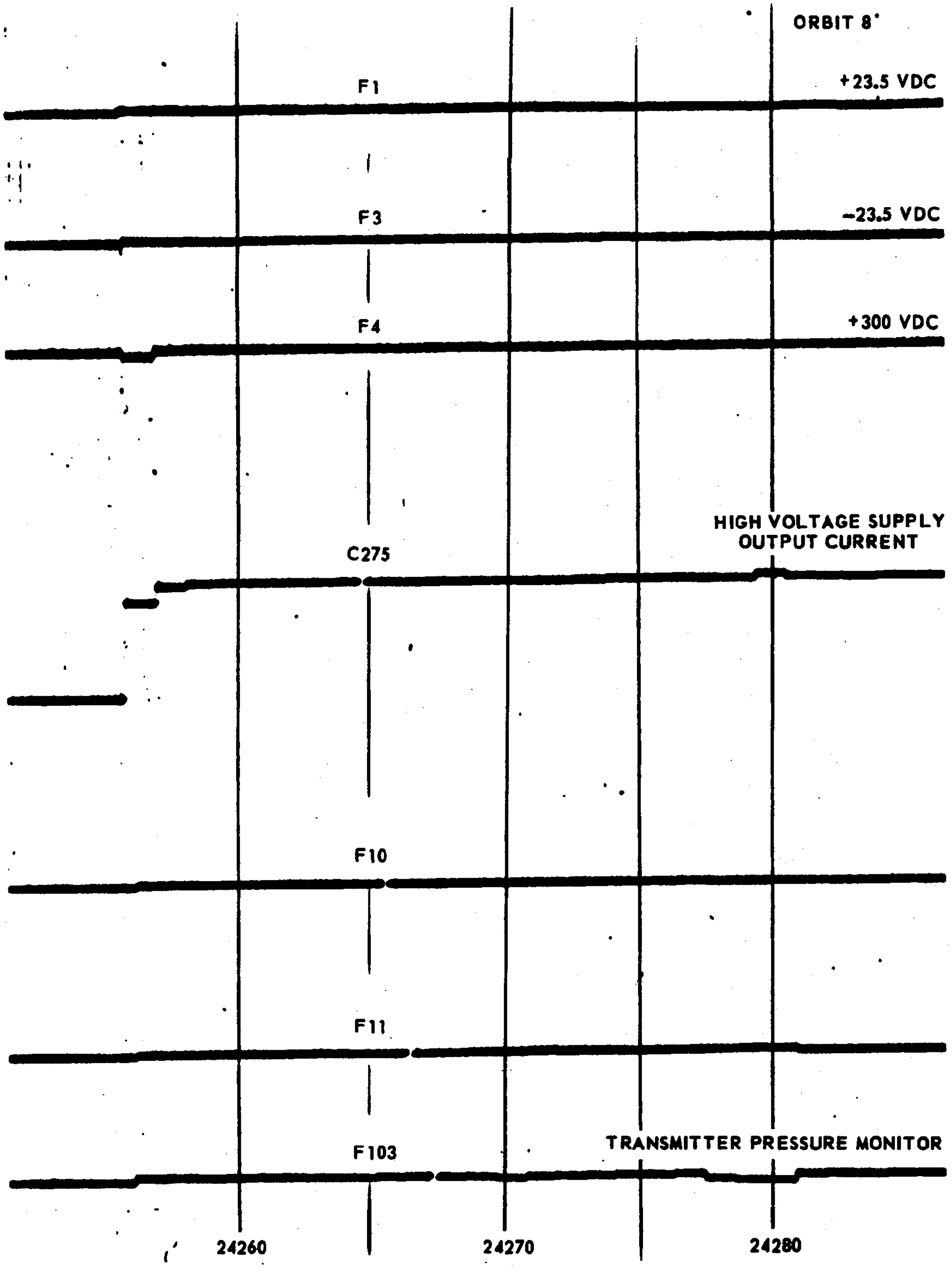
ORBIT 8
F1
+23.5 VDC
F3
-23.5 VDC
F4
+300 VDC
C275
HIGH VOLTAGE SUPPLY OUTPUT CURRENT
F10
F11
F103
TRANSMITTER PRESSURE MONITOR
24260
24270
24280

Figure 3.1.5

3.2 Attitude Control Subsystem

3.2.1 System Performance Summary

The two most significant aspects of the vehicle flight performance and subsequent evaluation were the extremely noisy horizon sensor signal outputs and the difficulty of extracting vehicle attitude pointing information from the payload data. The horizon sensor outputs exhibited noise to some extent on every active pass. In a few cases the anomalous sensor signals appeared to exceed 2° peak-to-peak. It should be noted that an anomalous horizon sensor output will not result in a corresponding vehicle attitude error. The relatively low horizon sensor to gyro torquing gains reduce the effect of the sensor signals and the error signal deadbands (about 0.35 average peak-to-peak) block out a large portion of the anomalous signal. One factor which tended to accentuate the anomalous horizon sensor performance on this flight was the improved telemetry resolution. Prior to the flight it had been thought that vehicle attitude could be extracted directly from the payload (radar map) data. This can (and has) been done for roll attitude but it now appears that this approach is impractical for pitch and yaw attitude data. This subject will be discussed in a subsequent section. Some attitude information apparently can be obtained through analysis of the payload system performance. It is expected that the Goodyear report will contain information on this subject.

In all other respects the control system performance was consistent with that predicted for the conditions of this flight. Items of particular interest are discussed in subsequent sections.

3.2.2 Derived Data-Vehicle

The Horizon Sensor output normally defines the vehicle's pitch and roll attitude. Unfortunately the Horizon Sensor output for this particular vehicle was anomalous. Part, if not all, of the cause for the erroneous Sensor output was the vast cold cloud cover at the time of the flight. At any rate, because of the loss of vehicle attitude data, some other means of determining vehicle attitude was necessary.

A number of methods were used. The initial attack was to approach the solution from a grossly approximate standpoint with the intent to refine the method as the results pointed to the most likely solution.

It was felt that the key to the solution lay in evaluating the impulse contained in each gas valve firing. In pursuit of this, the following method was used:

$$T = I\alpha \qquad (1)$$

$$FR = I\frac{\Delta W}{\Delta t} \qquad (2)$$

$$F\ t = \frac{I}{R}\Delta W \qquad (3)$$

$$\text{Impulse per pulse} = \frac{F\Delta t}{N} = i\ ;\ i_2;\ \ldots i_6 \qquad (4)$$

and it follows that

$$i_1 \propto W_1;\ i_2 \propto W_2;\ \text{etc.}$$

(see Figure 3.2.1 for gas valve location and vehicle axis description).

Vehicle body rates were obtained in the following manner:

$$W_y = \dot{\theta}_g - \dot{\theta}_d + \dot{\theta}_c - W_o - K_\theta (H_\theta - \theta_g) \qquad (5)$$

$$W_x = \dot{\phi}_g - \dot{\phi}_d + \psi\dot{\theta} \mp \dot{\phi}_c \pm \psi_c W_o - K_\phi H_\phi \qquad (6)$$

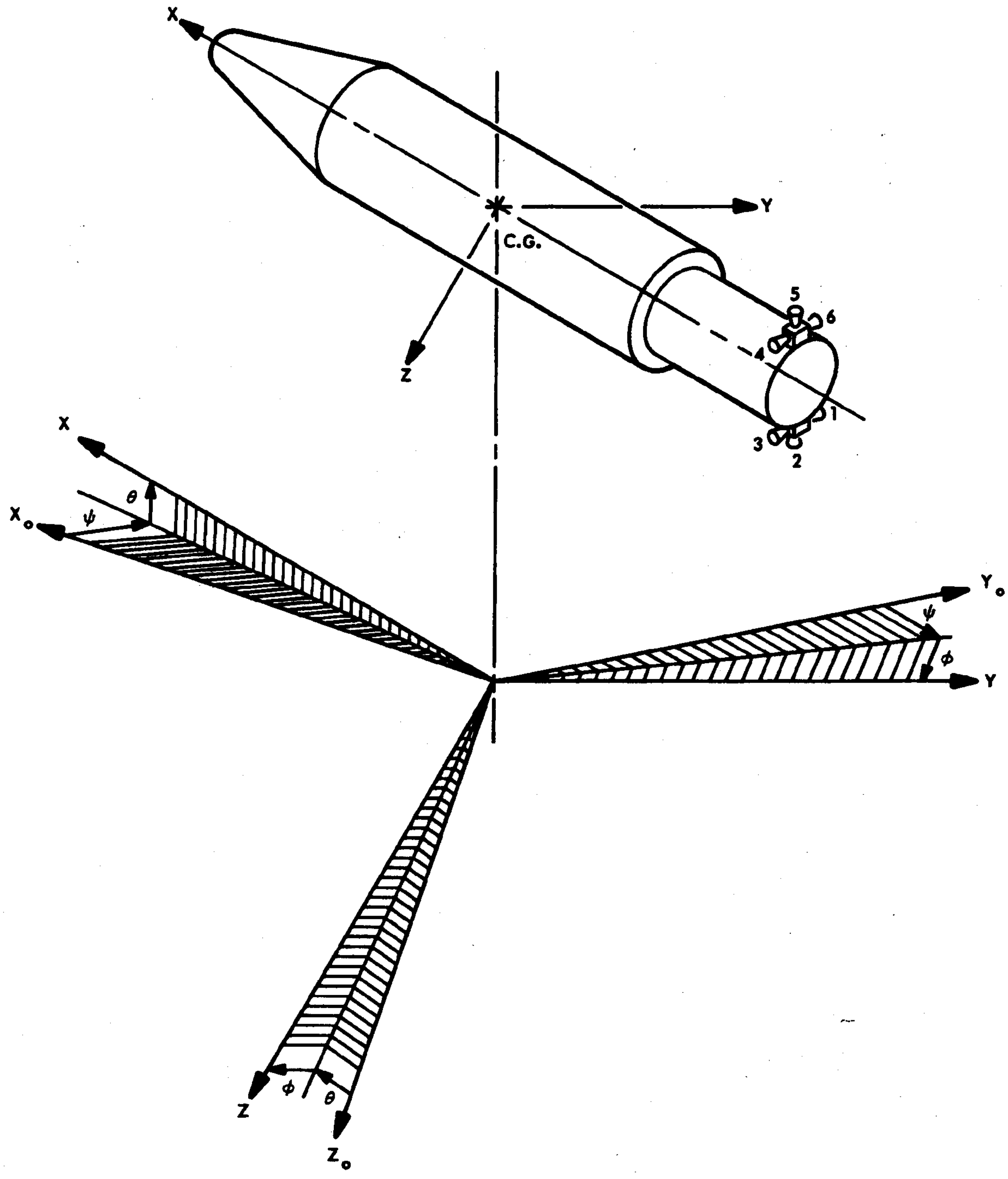

FIGURE 3.2.1 GAS VALVE LOCATION AND VEHICLE AXES

$$W_z = \dot{\psi}_g - \dot{\psi}_d - \phi\,\dot{\theta} + K_\psi \; H\,\phi \qquad (7)$$

Assuming:

1. Gyro drift rates are zero
2. $W_o = \dot{\theta}_c$
3. $\psi = \phi = 0$
4. $\mp \dot{\phi}_c = \pm \psi_c W_o$

The body rate equations become:

$$W_y = \dot{\theta}_g - K_\theta \,(H_\theta - \theta_g) \qquad (8)$$

$$W_x = \dot{\phi}_g - K_\phi \, H_\phi \qquad (9)$$

$$W_z = \dot{\psi}_g + K_\psi \; H_\phi \qquad (10)$$

The use of these equations also neglects such potential error sources as:

1. Horizon Sensor torquing gain tolerance
2. External torques
3. Telemetry linearity and bias uncertainty
4. Component alignment to body axis errors

and assumes:

1. Gyro rate thresholds are zero deg/sec.
2. Each gas valve command produces a valve firing

The first attempt using the above method produced rates per gas valve firing of 0.0006 deg/sec for the pitch and yaw axes. (For convenience, from now on in this report, rates will be stated in milli-degrees per second (m °/s): 0.0006 °/s = 0.6 m °/s).

While these rates per gas valve firing produced reasonable pitch and yaw rates and attitude changes, the roll rates and displacement were not reasonable. For this reason, rate calculations were performed for another pass. (By this time better data records were available.) The results were as follows:

$W_{z1} = W_{z6} = 0.62$ and 0.55 m °/s

$W_{z3} = W_{z4} = 0.46$ m °/s

$W_{y2} = 0.82$ and 0.64 m °/s

$W_{y5} = 0.85$ m °/s

These results indicated a greater dispersion in the rate produced per gas valve firing (W/VF) than had been anticipated. For this reason it was decided to concentrate on the non-coupled pitch axis W/VF for all of the thirteen passes available. The results produced the following range in the data:

$W_{y2} = 0.64$ to 1.14 m °/s

$W_{y5} = 0.75$ to 1.40 m °/s

The weighted average of the W/VF was:

$\overline{W_{y2}} = 0.80$ m °/s

$\overline{W_{y5}} = 0.92$ m °/s

The difference between the impulse from gas valve #2 and gas valve #5 could be real, or it could be caused by an external torque which tended to produce a positive rate. Sources of external torque would be:

1. Vehicle's magnetic moment interacting with the earth's magnetic field
2. Gravity gradient

3. Aerodynamic
4. Rotating machinery on board

The data were examined for the presence of an external torque. During times when the Horizon Sensor output was disconnected from the gyro, it was noted that in the absence of gas valve firings, rate changes occasionally appeared on the gyro outputs. The required torque to produce the rate change was calculated. Its value was found to be 0.0018 foot-pound. The gravity gradient moment would be of a magnitude of 0.00045 foot-pound per degree, and the aerodynamic moment would be 0.0028 foot-pound per degree. These are small values compared with the observed moment. Therefore the magnetic moment was assumed to be the major contributor to the apparent torque. In light of this, four passes, one day apart, were analyzed and evaluated. The reason for selecting them one day apart was to place each pass in essentially the same earth's magnet field, therefore the same magnetic moment.

Further, because of the wide variance in W/VF, that method of evaluation was temporarily abandoned. Pitch body rates were determined, and a steady state torque was superimposed upon these calculated rates. The rates were numerically integrated,and the curves shown in Figures 3.2.2 thru 3.2.5 were produced. The curves do exhibit similarities, but they do not suggest the possible vehicle attitude.

It was next decided to perform the same type of operation on the roll and yaw parameters for the same passes. It was felt that the pitch and roll sensor errors together might suggest a solution for vehicle attitude.

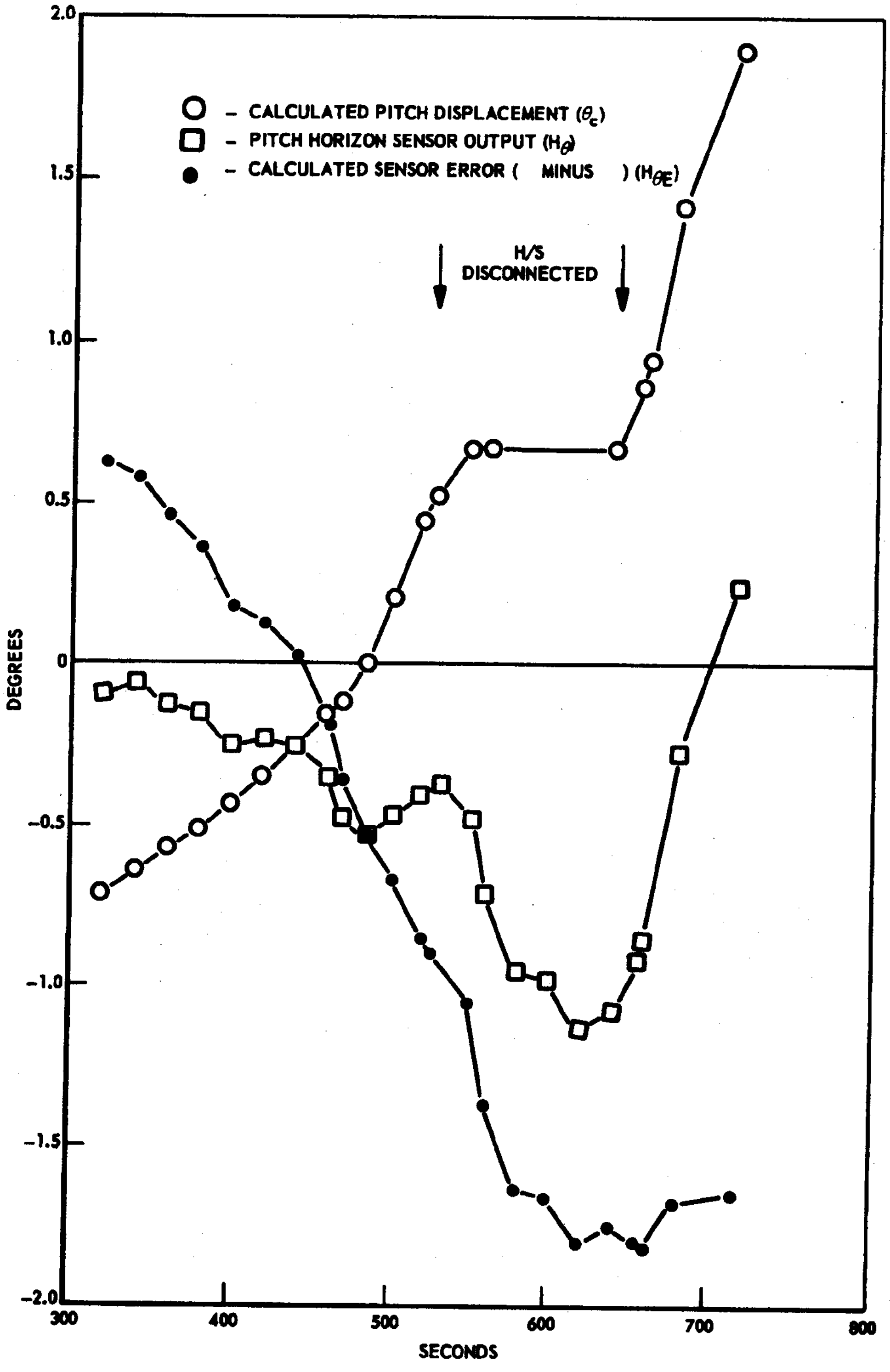

FIGURE 3.2.2 PITCH ATTITUDE VS. SYSTEM TIME (PASS 9)

NRO APPROVED FOR RELEASE
DECLASSIFIED BY: C/IART
DECLASSIFIED ON: 9 JULY 2012

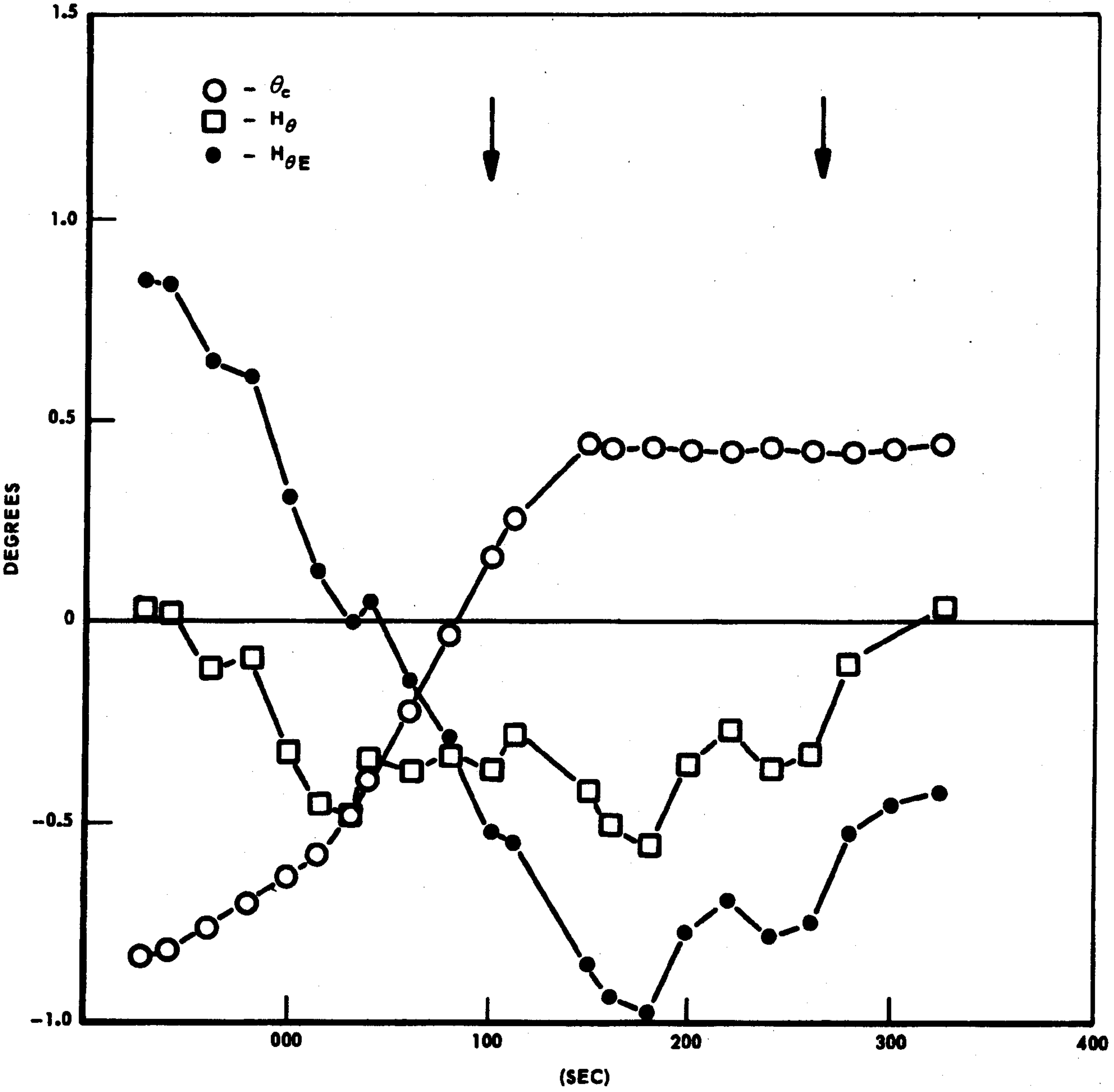

FIGURE 3.2.3 PITCH ATTITUDE VS. SYSTEM TIME (PASS 25)

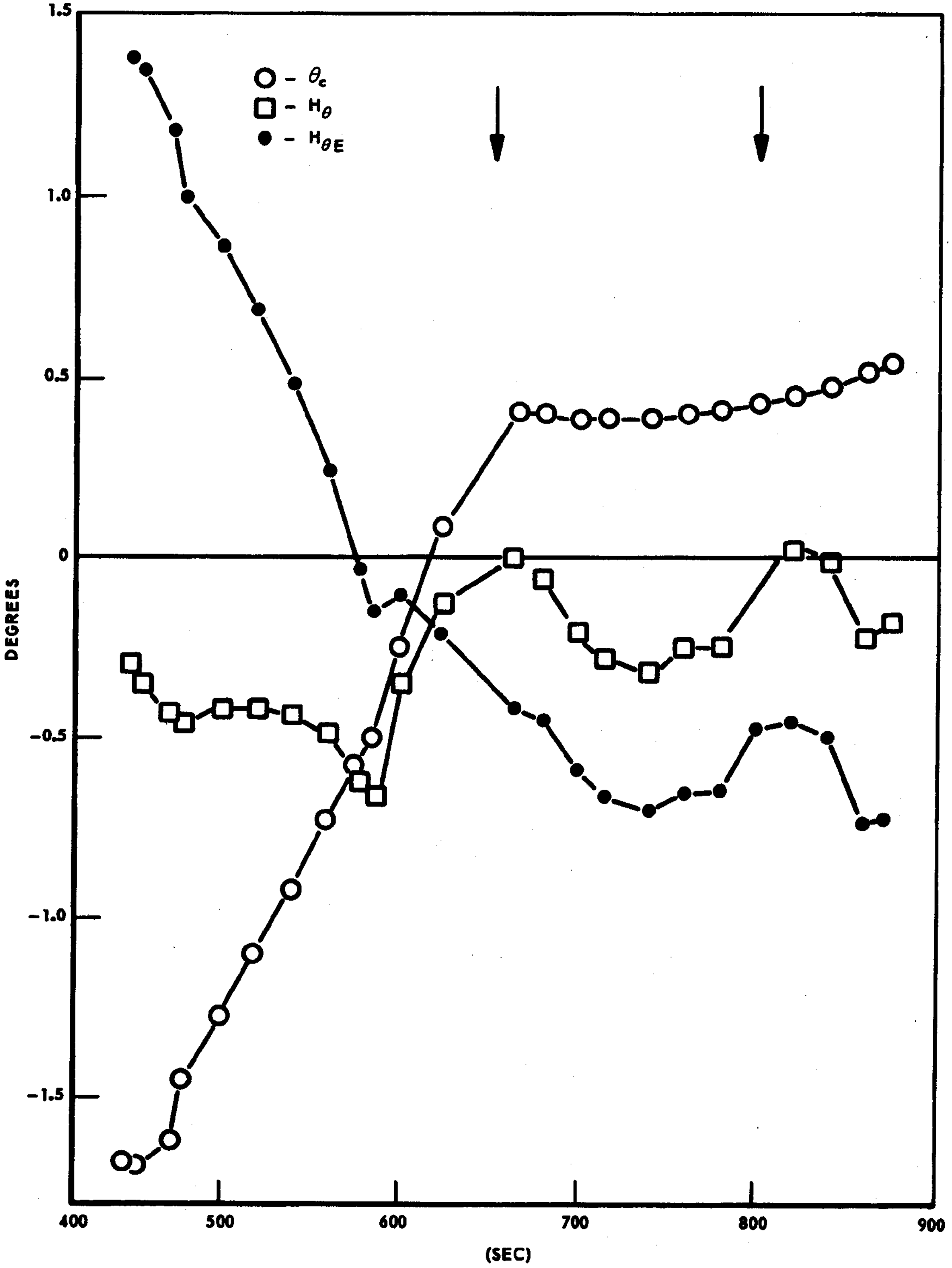

FIGURE 3.2.4 PITCH ATTITUDE VS. SYSTEM TIME (PASS 41)

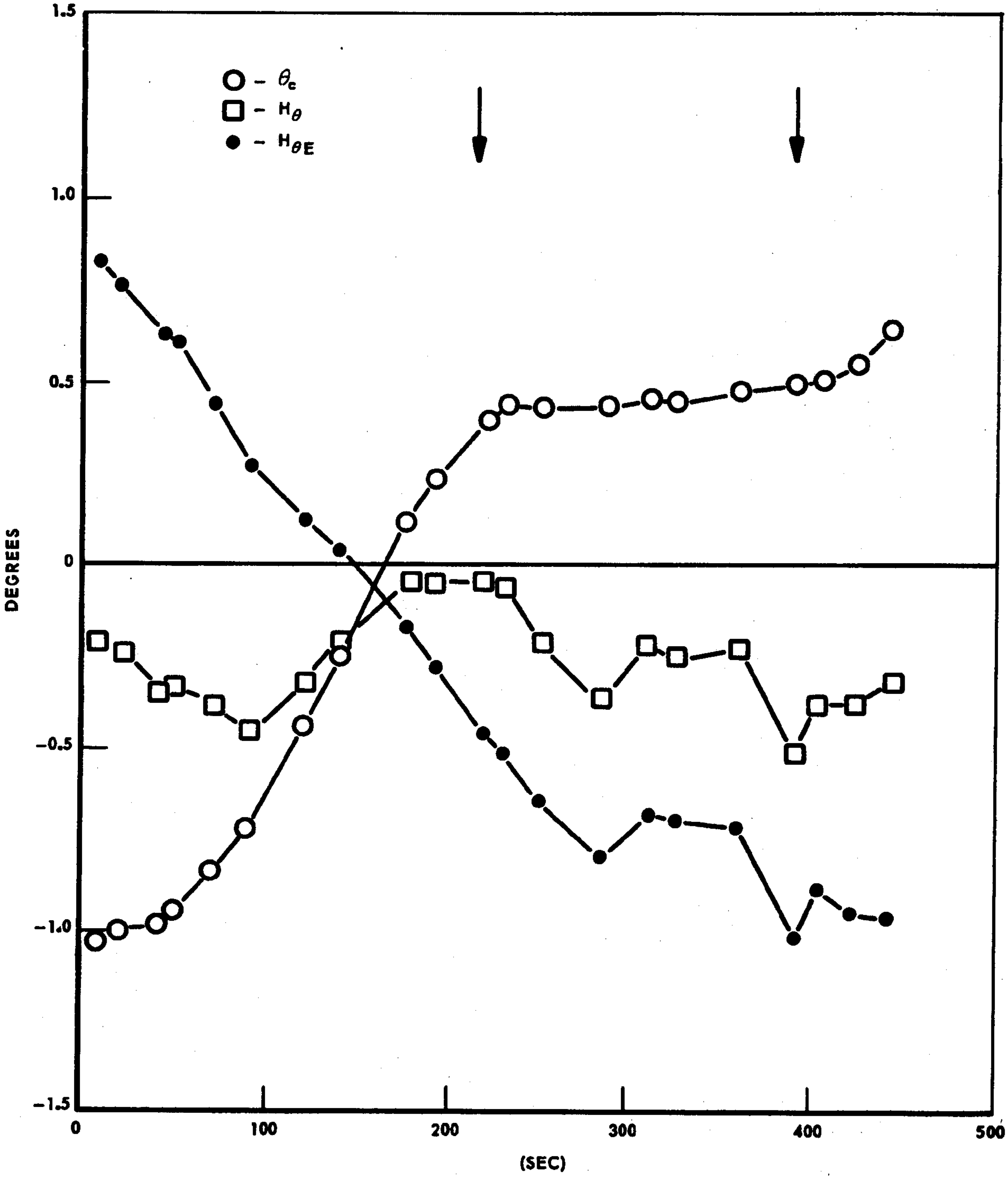

FIGURE 3.2.5 PITCH ATTITUDE VS. SYSTEM TIME (PASS 57)

Because roll rates (W_x) always appeared low, and thus more greatly affected by the absence of the ψW_o and $\dot{\phi}_d$ terms in the approximate eq. (9), it was decided to attempt again to evaluate W/VF.

The method used was:

$$N_1 W_{z1} + N_2 W_{z6} = (\Delta W_z)_1$$

$$N_3 W_{z1} + N_4 W_{z6} = (\Delta W_z)_2$$

Solving equations (11) and (12) simultaneously results in a solution for W_{z1} and W_{z6}. Similar solutions may be obtained for W_{z3} and W_{z4}. Rates produced about the yaw axis are related to the rates produced about the roll axis by the ratio of their respective inertias and lever arms.

Therefore:

$$W_x = 3.1\, W_z$$

and roll rate changes are:

$$(\Delta W_x)_1 = N_1 W_{x1} - N_2 W_{x6}$$

$$(\Delta W_x)_2 = N_5 W_{x3} - N_6 W_{x4}$$

The results obtained again indicated large variations in the W/VF value. The final attempt to arrive at a reasonable W/VF value utilized the following set of equations:

$$N_1 W_{z1} + N_2 W_{z6} = (\Delta W_z)_1$$

$$N_1 W_{x1} - N_2 W_{x6} = (\Delta W_x)_1$$

These equations were solved simultaneously. The results again were inconsistent. At this point the attempt to evaluate W/VF was abandoned.

Yaw displacements were calculated in the same manner as the pitch displacements had been. (Yaw rates are higher than roll rates so it was reasonable to exclude the ϕW_o and the $\dot{\psi}_d$ terms.) There was reason to believe that an external torque existed in yaw also. For this reason a steady state rate was superimposed on the calculated body rates. The curves produced are shown in Figures 3.2.6, 3.2.7, and 3.2.8. The yaw displacement did not exhibit the consistency from pass to pass observed on the pitch curves. It may be observed that the average yaw rates during Horizon Sensor disconnect are lower than the average yaw rates while the Horizon Sensor is connected. The average yaw displacement during these three passes was 0.84 degree. Using:

$$W_x = \psi W_o$$

The average change in roll rate due to this changing yaw attitude may be calculated. This average change was found to be 1.0 m °/s. This is too small a change to be useful in evaluating roll attitude.

The next approach, in an effort to obtain roll attitude, was to request from another subsystem a point in time when a yaw error was suspected. This data was then used in the following expression:

$$\dot{\phi} = \dot{\phi}_g + \psi \dot{\theta} - K_\phi H_\phi$$

This is essentially eq. (6). Data for Figure 3.2.9 were calculated. The plot without the "$\psi \dot{\theta}$" correction was also included on the figure. Neither plot exhibited good correlation with the roll output of the Horizon Sensor.

The last attempt to establish absolute attitude data was based upon the

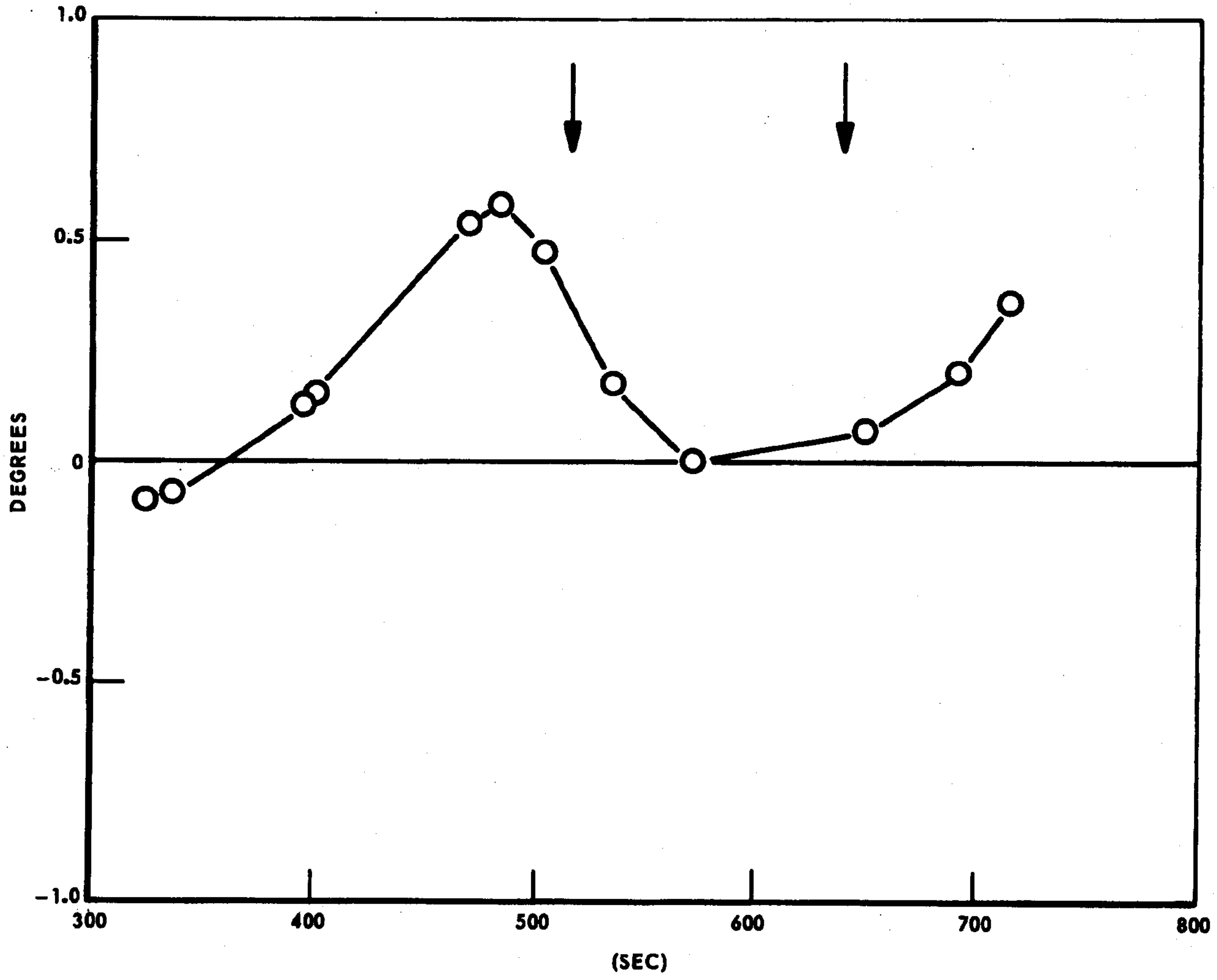

FIGURE 3.2.6 YAW DISPLACEMENT VS. SYSTEM TIME (PASS 9)

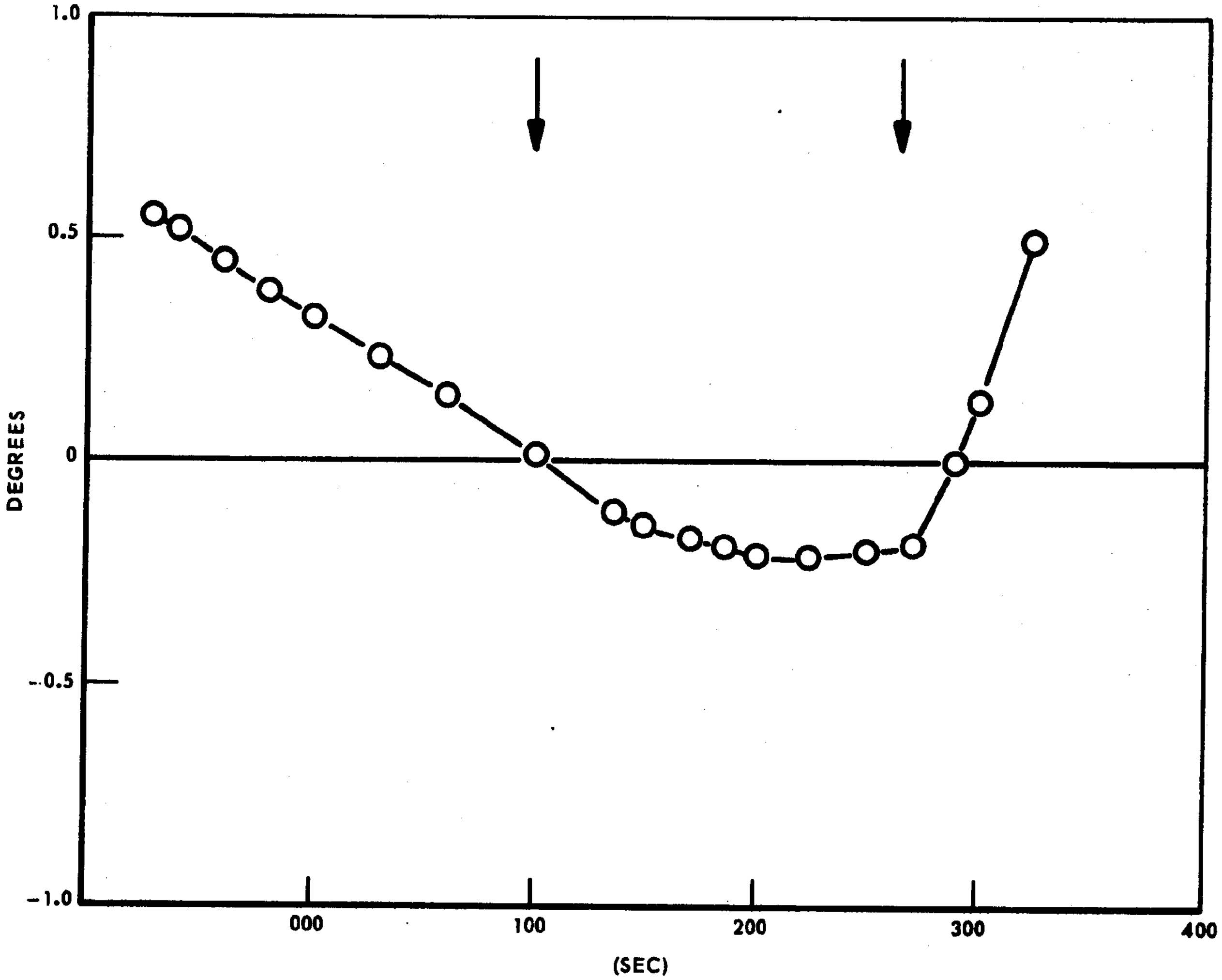

FIGURE 3.2.7 YAW DISPLACEMENT VS. SYSTEM TIME (PASS 25)

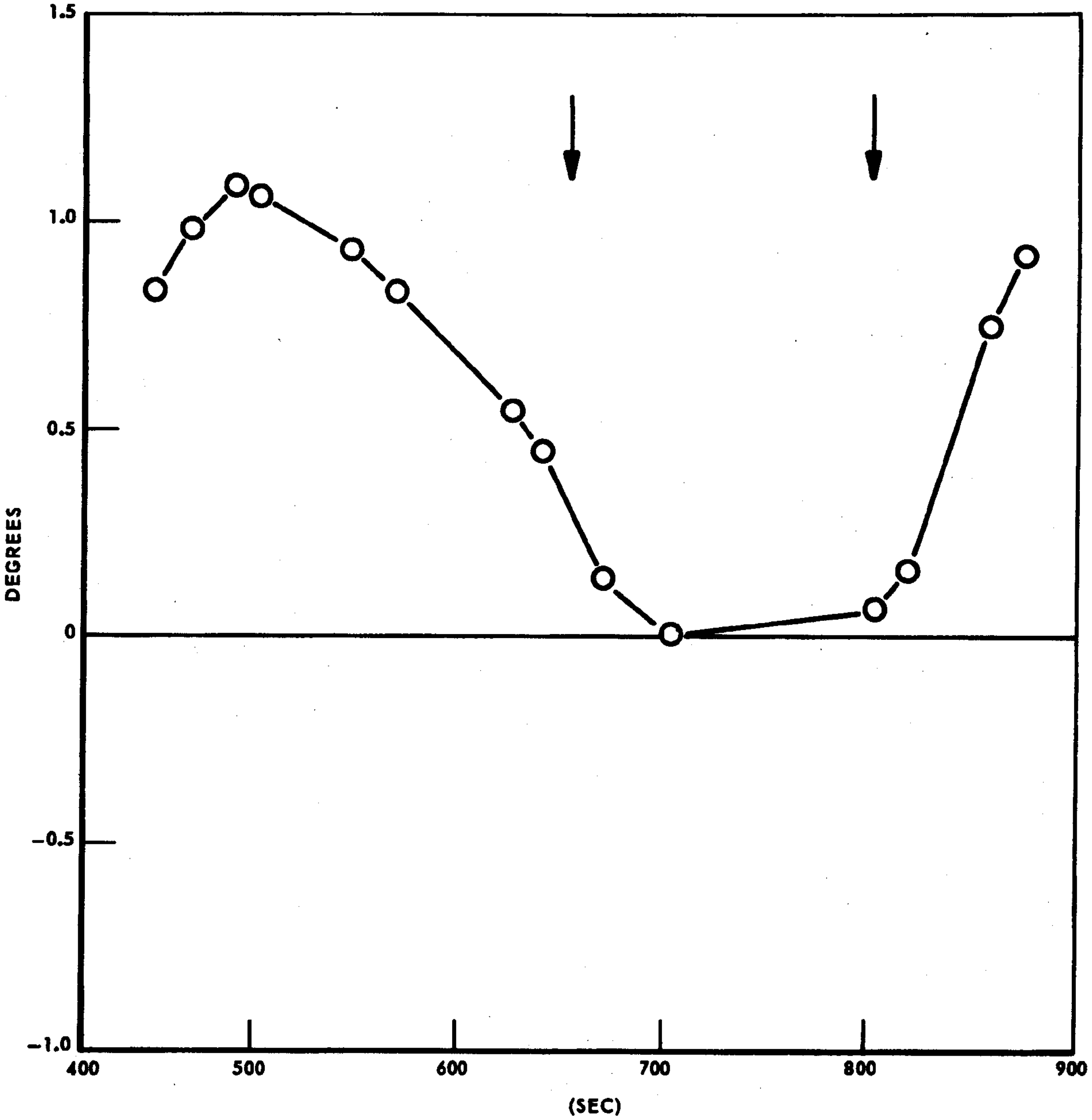

FIGURE 3.2.8 YAW DISPLACEMENT VS. SYSTEM TIME (PASS 41)

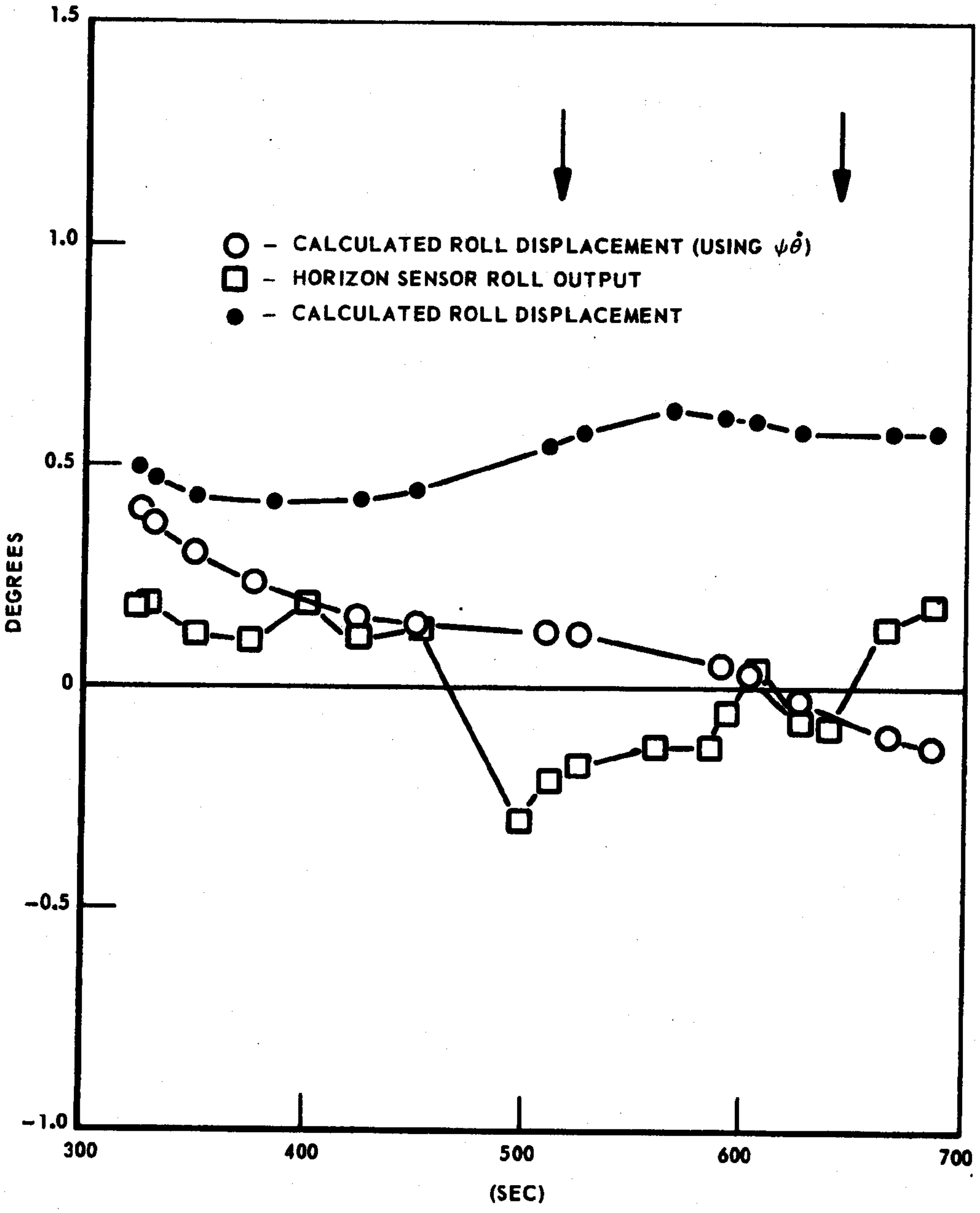

FIGURE 3.2.9 ROLL PARAMETERS VS. SYSTEM TIME (PASS 9)

premise that at sometime the Horizon Sensor output must be exhibiting true vehicle attitude. The data from all 13 passes were reviewed, and a pass which seemed to offer the best possibilities was chosen. Yaw displacement was backed out of eq. (18). The correlation with the yaw displacement which was calculated using eq. (10) was poor. It was at this point in time that further effort to obtain absolute roll and yaw attitude information was discontinued. The possibility of determining absolute pitch attitude using the latter method has promise. However, the value of this quantity is not as great as the roll - yaw parameters. Therefore this method was not pursued.

Pitch and yaw body rates have been evaluated. They are tabulated in Table 3.2.2. The confidence in this data is good. The pitch rate tabulated is body rate minus orbital rate. It should be noted that in almost every case the pitch and yaw body rates were quite high immediately following the horizon sensor disconnect. These rates resulted from the anomalous Horizon Sensor signals. When the corresponding attitudes attained an amplitude sufficient to actuate the pneumatic system these rates were damped to much lower levels. Thus if the first twenty seconds of each pass were ignored the average rates would be approximately one half of the values tabulated.

No attempt to evaluate roll rates was made for two reasons:

1. The magnitude of the roll rates were so low that the $\dot{\phi}d$ and the ψw_o terms became significant.
2. The threshold rate of the roll gyro was unknown.

The observed roll rates were well below the required limits in all cases.

TABLE 3.2.1

Definition of Symbols

Symbol	Description	Units
F	Thrust at the gas valve	lb
H_ϕ, H_θ	Horizon Sensor output	deg
$i_1; i_2; \dots i_6$	Gas valve #1, #2, ... #6 impulse per pulse	lb-sec/ pulse
I_x, I_y, I_z	Components of vehicle inertia	ft-lb-sec^2
K_ϕ, K_θ, K_ψ	Horizon Sensor to gyro torquing gains	deg/sec/ deg
$N_1; N_2; \dots N_3$	Number of gas valve firings	
R_x, R_y, R_z	Gas valve moment arm	ft
t	time	sec
x, y, z	components of body axes	
α	angular acceleration	rad/sec^2
ϕ, θ, ψ	Euler angles	deg
$\dot{\phi}$, $\dot{\theta}$, $\dot{\psi}$	Euler angle rates	deg/sec
ϕg, θg, ψg	Gyro angles	deg
$\dot{\phi} g$, $\dot{\theta} g$, $\dot{\psi} g$	Gyro angular rates	deg/sec
ϕc, θc, ψc	Commanded vehicle attitude	deg
$\dot{\phi} c$, $\dot{\theta} c$, $\dot{\psi} c$	Commanded vehicle rate	deg/sec
$\dot{\phi} d$, $\dot{\theta} d$, $\dot{\psi} d$	Gyro drift rate	deg/sec
W_o	Orbital pitch over rate	deg/sec
W_x, W_y, W_z	Vehicle body rates	deg/sec

TABLE 3.2.1 (Cont.)

Symbol	Description	Units
$\Delta W_x, \Delta W_y, \Delta W_z$	Change in vehicle body rates	deg/sec
$W_1; W_2; \ldots W_6$	Body rate produced per gas valve firing	deg/sec/ pulse
$W/_{VF}$	Body rate produced per gas valve firing	
↓ ↓	Start and End of payload operation	

TABLE 3.2.2

Pitch and Yaw Body Rates
During Horizon Sensor Disconnect

Pass	$\dot{\theta} - W_0$	W_z	Δt
8	0.0	2.89	120
9	1.97	2.98	124
14	1.68	2.92	124
16	0.49	4.05	96
24	3.03	2.74	130
25	1.55	1.50	166
30	1.59	2.36	223
40	0.14	2.98	109
41	0.21	2.50	146
46	1.81	0.62	194
47	1.92	2.62	179
56	3.20	1.22	105
57	0.41	2.47	172